Dipolar Correlation NMR Spectroscopy of a Membrane Protein

Janet M. Griffiths,[†,‡] K. V. Lakshmi,[†,§] Andrew E. Bennett,[†,‡] Jan Raap,[⊥] C. M. van der Wielen,[⊥] Johan Lugtenburg,[⊥] Judith Herzfeld,[§] and Robert G. Griffin*[,†,‡]

Contribution from the Francis Bitter National Magnet Laboratory, Massachusetts Institute of Technology, Cambridge, Massachusetts 02139, Department of Chemistry, Massachusetts Institute of Technology, Cambridge, Massachusetts 02139, Department of Chemistry, Brandeis University, Waltham, Massachusetts 02254, and Department of Chemistry, Rijksuniversiteit te Leiden, NL-2300 R A Leiden, The Netherlands

Received May 17, 1994[⊛]

Abstract: We demonstrate the application of a new NMR experiment—RF-driven recoupling (RFDR)—for establishing spatial connectivities and measuring internuclear distances in spinning solids. RFDR employs rotor-synchronized π-pulses in a longitudinal mixing scheme to reintroduce dipolar couplings into magic angle spinning (MAS) NMR experiments. We have utilized this technique to measure a 0.25 nm distance in polycrystalline D,L-alanine and to determine relative distances in the integral membrane protein bacteriorhodopsin (bR). In the latter case, we have focused on an internuclear distance that defines the configuration about the retinal–protein Schiff base linkage in the two conformers comprising dark-adapted bR. Our results demonstrate that RFDR is a valid and practical technique for structural investigations of solids including biological molecules with molecular weights as great as 85 kDa.

Introduction

The development of high-resolution NMR techniques for determining the three-dimensional (3D) structure of macromolecules is an important focus in biophysics. Solution NMR techniques which rely on the observation of dipolar cross-relaxation (nuclear Overhauser enhancement spectroscopy) or coherence transfer via J-couplings have evolved to the point where molecular structures as great as ~25 kDa are readily solved.[1] However, these techniques are ineffective for large classes of molecules that are immobilized in cell membranes, complexed with other molecules, or tumble slowly. In the present study, we demonstrate a new high-resolution solid state NMR experiment—RF-driven recoupling (RFDR)—for establishing spatial connectivities and for measuring distances in these systems.[2]

The RFDR experiment employs a rotor-synchronized π-pulse train in a longitudinal exchange experiment to recouple the homonuclear dipole–dipole interaction. Although the dipole coupling is a strong function of internuclear distance, its magnitude is usually difficult to measure in complex molecules where multiple couplings are present, or where distances are long. It is therefore necessary to employ magic angle spinning (MAS) to achieve high-resolution spectra, and to recover the dipolar couplings of interest using a suitably engineered pulse scheme. A number of these recoupling schemes have been developed over the past 5 years, including rotational resonance (R^2),[3] DRAMA,[4] USEME,[5] SEDRA,[6] and RFDR. Among these experiments, RFDR offers a number of important advantages because of its suitability for 2D homonuclear dipolar correlation spectroscopy.

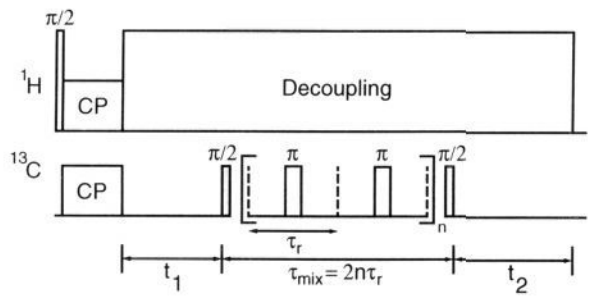

Figure 1. The 2D RFDR pulse sequence. Initial ^{13}C magnetization is generated with a cross-polarization pulse, followed by an evolution period (t_1). A single, non-selective $\pi/2$-pulse creates longitudinal magnetization. Rotor-synchronized π-pulses are applied once per rotor period (τ_r) during the mixing time τ_m. The π-pulses are phase alternated according to the XY-16 scheme XYXYYXYX (XYXYYXYX)$^{-1}$ to minimize the influence of resonance offset effects and other pulse errors.[22] A second non-selective $\pi/2$-pulse generates observable magnetization which is recorded during t_2. In the 1D version of RFDR, the t_1 period is replaced with a selective inversion pulse, or DANTE[23] sequence.

Figure 1 shows a diagram of the pulse sequence for 2D RFDR in which a train of RF π-pulses generates an effective dipolar flip–flop coupling term ($I_+S_- + I_-S_+$). A key feature of the experiment is the use of a longitudinal mixing scheme—where magnetization is placed along the axis of the magnetic field—which facilitates transfer of polarization among dipolar coupled spins. A second important feature is that chemical shift terms, which are refocussed by the π-pulse train, interfere with the amplitude modulation of dipole–dipole couplings by MAS, thereby allowing efficient reintroduction of homonuclear dipolar interactions across a broad range of chemical shift differences. RFDR can be performed as a one-dimensional (1D) experiment where the mixing period (τ_m) is incremented and the magnetization exchange between spins, recorded as a function of τ_m, maps out the dipole–dipole coupling strength. The two-dimensional (2D) version of RFDR utilizes an evolution period t_1, during which the spin system evolves according to its chemical shifts, followed by

† Francis Bitter National Magnet Laboratory, Massachusetts Institute of Technology.
‡ Department of Chemistry, Massachusetts Institute of Technology.
§ Brandeis University.
⊥ Rijksuniversiteit te Leiden.
⊛ Abstract published in *Advance ACS Abstracts,* October 1, 1994.

(1) See, for example: (a) Clore, G. M.; Gronenborn, A. M. *Annu. Rev. Biophys. Chem.* **1991**, *21*, 29. (b) Wuthrich, K. *Science* **1989**, *243*, 45.

(2) (a) Bennett, A. E.; Ok, J. H.; Griffin, R. G.; Vega, S. *J. Chem. Phys.* **1992**, *96*, 8634. (b) Sodickson, D. K.; Levitt, M. H.; Vega, S.; Griffin, R. G. *J. Chem. Phys.* **1993**, *98*, 6742–6748.

(3) (a) Raleigh, D. P.; Creuzet, F.; Gupta, S. K. D.; Levitt, M. H.; Griffin, R. G. *J. Am. Chem. Soc.* **1989**, *111*, 4502–4503. (b) Colombo, M. G.; Meier, B. H.; Ernst, R. R. *Chem. Phys. Lett.* **1988**, *146*, 189–195. (c) Levitt, M. H.; Raleigh, D. P.; Cruezet, F.; Griffin, R. G. *J. Chem. Phys.* **1990**, *92*, 6347–6364.

(4) (a) Tycko, R.; Dabbagh, G. *Chem. Phys. Lett.* **1990**, *173*, 461–465. (b) Tycko, R.; Smith, S. O. *J. Chem. Phys.* **1993**, *98*, 932–943.

(5) (a) Ramamoorthy, A.; Fujiwara, T.; Nagayama, N. *J. Magn. Reson. Ser. A* **1993**, *104*, 366. (b) Fujiwara, T.; Ramamoorthy, A.; Nagayama, K.; Hioka, K.; Fujito, T. *Chem. Phys. Lett.* **1993**, *212*, 81.

(6) Gullion, T.; Vega, S. *Chem. Phys. Lett.* **1992**, *194*, 423–428.

0002-7863/94/1516-10178$04.50/0

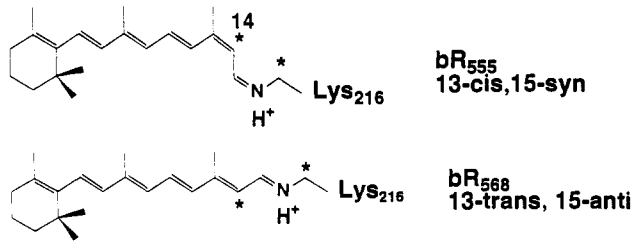

Figure 2. Illustration of the retinal chromophore conformations in dark-adapted bR: bR_{555} is 13-cis, 15-syn, and bR_{568} is 13-trans, 15-anti. ^{13}C-labeled sites are indicated by an asterisk. The Schiff base is protonated in both conformers.

a variable mixing time, τ_m. The resulting spectra resemble 2D solution correlation spectra obtained via nuclear Overhauser enhancement spectroscopy (NOESY)[7] and total correlation spectroscopy (TOCSY).[8] However, the accuracy of distances reported by RFDR is potentially greater because the direct dipole couplings utilized in solid-state experiments are a larger effect than indirect cross-relaxation utilized in solution NMR spectroscopy. In practice, distances up to ~0.5 nm (corresponding to couplings of ~60 Hz) are accessible for ^{13}C spin pairs, while the range may be considerably longer for ^{31}P, ^{1}H, and other high γ nuclei.[9]

We first demonstrate the 1D RFDR experiment for ^{13}C-labeled D,L-alanine, where the dipolar coupling strength was determined by recording the change in spectral intensity of the $^{13}CO_2$ and $^{13}CH_3$ lines as a function of mixing time.

In a second study, we used 2D ^{13}C RFDR spectroscopy to examine the conformation of the retinal–protein linkage in bacteriorhodopsin (bR). This 26 kDa membrane protein, which uses light to create an electrochemical proton gradient in *Halobacterium halobium*, has received considerable attention as a model system for elucidating the molecular basis of active transport in biophysical systems.[10] The active site of the protein is a retinal chromophore positioned near the center of a bundle of seven transmembrane α-helices and linked to Lys_{216} by a Schiff base. Two conformers, bR_{555} and bR_{568}, coexist in dark-adapted bR. bR_{568} is also the sole conformer in light-adapted bR, and proton translocation is initiated upon absorption of a photon by the all-trans retinal in this species. Rapid isomerization of the retinal to the 13-cis form ensues, yielding a series of short-lived photointermediates characterized by changes in conformation and protonation at the chromophore and in the surrounding protein. In the course of the photocycle, a proton is released to the extracellular space and replaced by another proton from the intracellular compartment.

A determination of the retinal conformation in the dark-adapted state and at each stage of the photocycle will provide important details for elucidating the role of retinal isomerizations in regulating proton transport in bR. For this purpose, we have prepared a sample of bR selectively labeled at two sites—[14-^{13}C]retinal and [ϵ-^{13}C]Lys216. This distance spans three bonds and provides an unambiguous measurement of the configuration (*syn* or *anti*) of the Schiff base C=N bond, as illustrated in Figure 2.

Experimental Section

Alanine Sample Preparation. This sample was prepared by dilution of 1,3-^{13}C-labeled D,L-alanine with a 9-fold excess of natural abundance alanine followed by slow recrystallization from aqueous solution. This dilution level was sufficient to minimize intermolecular ^{13}C couplings.

bR Sample Preparation. [ϵ-^{13}C,^{15}N]Lys was synthesized according to the procedure of Raap *et al.*[11] and was incorporated into the bR in the JW-3 strain of *Halobacterium halobium* as described previously.[12] The ^{15}N label was introduced in order to remove the line broading of the ϵ-^{13}C Lys resonance line by the quadrupolar ^{14}N nucleus. Unlabeled retinal was removed by bleaching the sample in 0.5 M hydoxylamine hydrochloride (pH 8) at 36 °C for 24 h in darkness. Freshly bleached bR was regenerated with [14-^{13}C]retinal by adding a 10% excess of retinal to the protein and storing the combined aqueous solution in the dark at 10 °C for 12 h. The extent of regeneration was monitored with UV/vis absorption; *i.e.* the peak at 560 nm corresponding to bound retinal was monitored relative to the peak at 350 nm corresponding to free retinal. The final extent of regeneration was 88%. Excess retinal was removed by repeated washing with deionized water and bovine serum albumin (BSA). Further repeated washing used 10 mM NaN_3 to remove BSA. To prepare for NMR experiments, the bR sample was washed in deionized water and centrifuged for 60 min at 30 000 g. The centrifuged pellet was packed in a 7 mm sapphire rotor for magic angle spinning. Regenerated samples were stored at 10 °C.

NMR Experimental Procedures. Carbon-13 NMR spectra were recorded at 79.85 MHz. Alanine data were collected using a ^{1}H $\pi/2$-pulse of 2.8 μs and a non-selective ^{13}C $\pi/2$-pulse of 4.0 μs. Mixing π-pulses were set at a lower field strength than non-selective $\pi/2$-pulses to minimize depolarization via the proton decoupling field. For this reason we have used relatively weak ^{13}C $\pi/2$ pulses of 20 μs. For the 2D RFDR spectra of bR, ^{1}H $\pi/2$-pulses were 4.4 μs, the non-selective ^{13}C $\pi/2$-pulse was 5.0 μs, and the mixing π-pulses were 22 μs. All samples were spun in a home-built NMR probe equipped with a standard MAS assembly (Doty Scientific, Columbia, SC).

For the 2D RFDR spectra, eighteen t_1 increments were used in the first dimension (F_1) with a spectral window of ±4.8 kHz, and 1024 points were recorded in the second dimension (F_2) with a spectral window of ±25 kHz. Some aliasing of carbonyl peak and sidebands occurs in F_1 as a consequence of the narrow spectral limits, but into regions that do not interfere with the formation or resolution of cross-peaks. A total of 3800 transients were recorded for each t_1 increment. Real and imaginary phase spectra were recorded separately according to the pure phase method of States *et al.*[13] The accumulated FID was subjected to a double Fourier transform (FT) yielding a single 2D absorption mode spectrum. 2D data sets were processed by applying an exponential line-broadening function of 50 Hz prior to Fourier transformation. A linear prediction algorithm was used to extrapolate from 18 points to 36 points in t_1, and this new array was zero filled to 1024 points prior to the second FT. A sample rotation rate of 3.200 kHz was utilized in order to facilitate optimum polarization transfer in the RFDR experiment.[2]

Results

Magnetization exchange spectra for [1,3-$^{13}C_2$]alanine are given in Figure 3A for a sample rotation rate of 4.800 kHz. Here, the $^{13}CO_2$ line was selectively inverted and the magnetization exchange between $^{13}CO_2$ and $^{13}CH_3$ was detected by the change in intensity of the two spectral lines as a function of τ_m. Simulation results, based on an exact numerical calculation for the 2-spin system under the action of π-pulses,[9] are shown in Figure 3B for a distance of 0.25 nm. Details of the simulations are described below.

Figure 4 shows the 2D RFDR spectrum of [14-^{13}C]retinal, [ϵ-^{13}C,^{15}N]Lys-bR, recorded with τ_m = 15 ms. The corresponding 1D CPMAS spectrum, which borders the 2D spectrum, shows the resonance lines for [ϵ-^{13}C]Lys_{216} at 48 and 53 ppm and for [14-^{13}C]retinal at 110 and 122 ppm in bR_{555} and bR_{568}, respectively.[14] The line at 40 ppm is due to the six Lys residues which are also ^{13}C enriched during the biosynthetic labeling of the sample. The remaining spectral lines can be attributed to the 1.1% natural abundance ^{13}C nuclei in the protein, retinal, and surrounding lipid. The diagonal in the 2D spectrum (including rotational sidebands spaced at the rotor frequency $\omega_r/2\pi$ = 3.2

(7) (a) Jeener, J.; Meier, B. H.; Bachmann, P.; Ernst, R. R. *J. Chem. Phys.* **1979**, *71*, 4546. (b) Wuthrich, K. *NMR of Proteins and Nucleic Acids*; Wiley Press: New York, 1986.
(8) Braunschweiler, L.; Ernst, R. R. *J. Magn. Reson.* **1983**, *53*, 512.
(9) Bennett, A. E.; Griffiths, J. M.; Griffin, R. G., unpublished results.
(10) (a) Henderson, R.; Baldwin, J. M.; Ceska, T. A.; Zemlin, F.; Beckman, E.; Downing, K. H. *J. Mol. Biol.* **1990**, *213*. (b) Mathies, R. A.; Lin, S. W.; Ames, J. B.; Pollard, W. T. *Annu. Rev. Biophys. Chem.* **1991**, *20*, 491.
(11) Raap, J.; van der Wielen, C. M.; Lugtenburg, J. *Recl. Trav. Chim. Pays-Bas* **1990**, *109*, 277.
(12) Argade, P. V.; Rothschild, K. J.; Kawamoto, A. H.; Herzfeld, J.; Herlihy, W. C. *Proc. Natl. Acad. Sci. U.S.A.* **1981**, *78*, 1643.
(13) States, D. J.; Haberkorn, R. A.; Ruben, D. J. *J. Magn. Reson.* **1982**, *48*, 286.
(14) Farrar, M. R.; Lakshmi, K. V.; Smith, S. O.; Brown, R. S.; Raap, J.; Lugtenburg, J.; Griffin, R. G.; Herzfeld, J. *Biophys. J.* **1993**, *65*, 310.

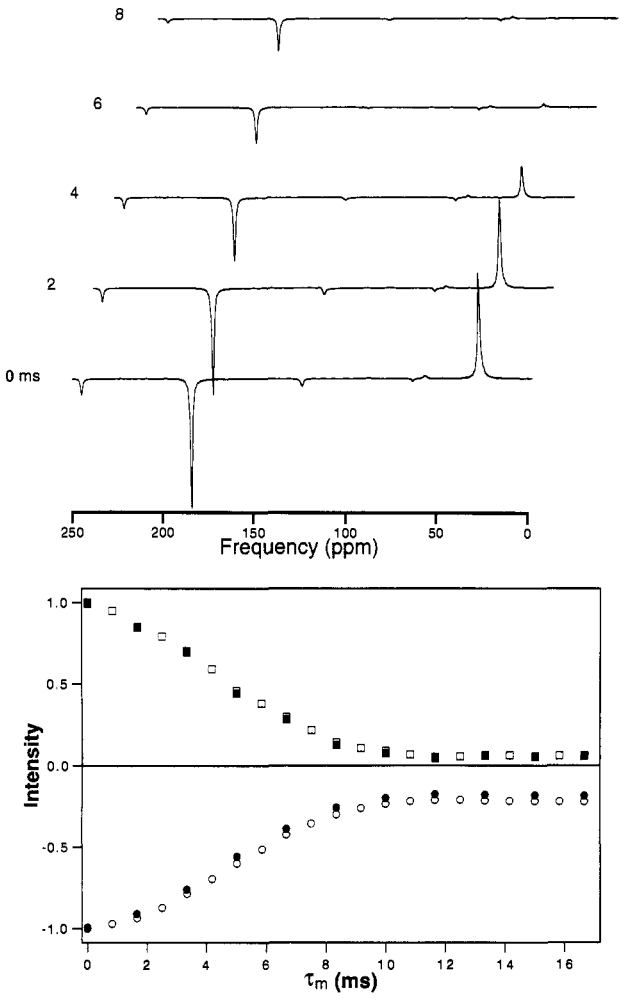

Figure 3. (A, top) 1D RFDR exchange spectra for D,L-[1,3-$^{13}C_2$]alanine at ω_r = 4.800 kHz with selective inversion of the $^{13}CO_2$ resonance line. (B, bottom) Experimental (solid symbols) and numerical (open symbols) intensities are given by squares for $^{13}CH_3$ and by circles for $^{13}CO_2$. The numerical simulation is for a distance of 0.251 nm. Spectra were recorded at 24 °C.

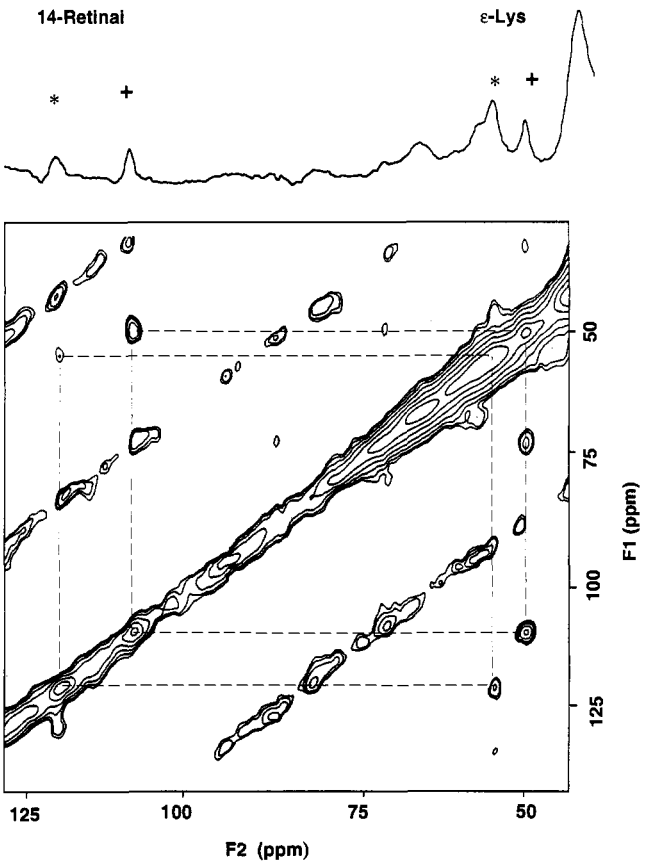

Figure 4. The 1D ^{13}C CPMAS spectrum of [14-^{13}C]retinal, [ε-^{13}C, ^{15}N]-Lys-bR shows resonance peaks arising from selectively enriched sites at 48 and 53 ppm for [ε-^{13}C]Lys_{216}, at 110 ppm and 122 ppm for [14-^{13}C]retinal, and at 40 ppm for free Lys residues. Signals specific to bR_{555} (bR_{568}) are identified by + (*). The 2D contour spectrum, recorded with τ_m = 15 ms, exhibits cross-peaks showing spatial connectivities between dipolar coupled nuclei. The sample rotation rate was $\omega_r/2\pi$ = 3.200 kHz; corresponding sidebands appear in the 2D spectrum displaced from the diagonal by this amount. A sample temperature of –60 °C was maintained throughout the experiments.

kHz) and the two pairs of cross-peaks corresponding to the selectively enriched sites are prominent features of the 2D landscape. Cross-peaks between sidebands and centerbands are also evident owing to the slow spinning rate and large sheilding anisotropy of the [14-^{13}C] spectral lines. Appearance of dipolar cross-peaks demonstrates that magnetization has exchanged between the dipole-coupled ^{13}C spins. A 2D spectrum of the same sample was also recorded in the absence of mixing pulses (τ_m = 0) and differs from the spectrum of Figure 4 in that cross-peaks are absent, thus confirming that the origin of the cross-peaks is due to dipolar exchange. Individual cross-peaks observed in this 2D spectrum correspond to a single pair of ^{13}C spins in a system with an effective molecular weight of ~85 kDa.[15]

Discussion

The rate of magnetization exchange during RFDR depends upon the magnitude of the dipole–dipole coupling, the chemical shift anisotropies, the tensor orientations, and the relaxation parameters of relevant spins. In most cases, an accurate measurement or reasonable estimation of these parameters is feasible. Chemical shift tensor elements for each spectral line were measured from MAS rotational sideband intensities using standard methods[16] and are reported elsewhere for the bR sample.[17] The relative orientations of the chemical shift and dipolar tensors were estimated from the geometries of both systems.[18]

Although T_2^{ZQ} dephasing does not induce signal losses in RFDR since the magnetization is stored longitudinally, this relaxation mode can slow the rate of dipolar exchange. Zero-quantum (T_2^{ZQ}) processes originate from dipolar interactions with natural abundance nuclei, incomplete proton decoupling, and molecular motion. We obtained an estimate of the zero-quantum dephasing rate using a transverse echo experiment. For [1,3-$^{13}C_2$]alanine, the effective T_2^{ZQ} rate was ~32 ms. In the bR system, the T_2^{ZQ} relaxation parameter was long compared to anticipated coupling strengths and, therefore, could be neglected in the simulation.

A decay parameter was also introduced to characterize the signal losses which arise from the dephasing of ^{13}C magnetization by insufficient proton decoupling during τ_m. Signal losses were distinguished from exchange by examining the decay rate of each resonance line during the 1D RFDR experiment in the absence of an inversion pulse. For $^{13}CO_2$ and $^{13}CH_3$ spectral lines in

(15) The bR protein, which has a molecular weight of 26.6 kDa, resides in a membrane that is 25% lipid. The effective molecular weight of the protein is therefore ~35 kDa. Of the two conformers comprising the dark-adapted form, bR_{568} accounts for 0.4 and bR_{555} accounts for 0.6 of the protein by weight, yielding an effective molecular mass of ~85 kDa for bR_{568}.

(16) Herzfeld, J.; Berger, A. E. *J. Chem. Phys.* **1980**, *73*, 6021.
(17) Thompson, L. M.; McDermott, A. E.; Raap, J.; van der Wielen, C. M.; Lugtenburg, J.; Herzfeld, J.; Griffin, R. G. *Biochemistry* **1992**, *31*, 7931–7938.
(18) (a) Mehring, M. *Principles of High-Resolution NMR in Solids*, 2nd ed.; Springer: New York, 1983. (b) Veeman, W. *Phil. Trans. R Soc. London* **1981**, *A299*, 629.

alanine, signal losses account for ~15% of the magnetization at τ_m = 15 ms. For the relevant spectral lines in bR, signal losses reached ~35% at τ_m = 15 ms. In both systems, signal losses were included explicitly in the spin dynamics calculation. The best fit to the exchange data in Figure 3B corresponds to a distance of 0.25 ± 0.01 nm, which is in excellent agreement with the crystallographic distance of 0.252 nm.[19]

The extent of magnetization exchange in a 2D experiment is reported by cross-peak intensity. In Figure 4, cross-peaks associated with bR_{555} have greater intensity than cross-peaks associated with bR_{568} and indicate a stronger dipolar coupling (shorter distance) in bR_{555}. Further information is supplied by performing numerical simulations. For this system, however, separate simulations were performed for the two spin pairs; dipolar exchange between the two pairs of peaks is not correlated because each conformer represents a separate and dilute spin system. The simulations, shown in Figure 5, correspond to distances of 0.31 and 0.39 nm for bR_{555} and bR_{568}, which are suggested by energy minimization calculations for the *syn* and *anti* conformations. Final simulation results were scaled to a ratio of 0.6:0.4 to coincide with the relative equilibrium populations of the two conformers. In Figure 5, where the magnetization originates at the ε-Lys spectral line, the predicted cross-peak intensity is 0.17 in bR_{555} and 0.09 in bR_{568} (ratio = 1.86) at τ_m = 15 ms. Upon integration of the cross-peak areas, we obtain a ratio of 1.9 (bR_{555}/bR_{568}) for magnetization originating on the ε-Lys lines (upper left-hand quadrant) and 1.6 for magnetization originating on 14-retinal lines (lower right-hand quadrant). Simulations for the case of magnetization originating at the 14-retinal line also predict a ratio of 1.9. The ratios measured in Figure 4 are therefore in close agreement with the ratios predicted by simulation.

Finally, we note that quantitative distances can be determined by measuring the intensity of the corresponding diagonal lines and normalizing these numbers to τ_m = 0. This approach was impractical in this system due to spectral congestion in the diagonal band. Difference spectroscopy, wherein spectra of a natural abundance sample are subtracted from spectra of the labeled sample, may be the best way to address this problem. Nevertheless, the relative distance measurements obtained with RFDR are consistent with the distances reported by rotational resonance (R^2) NMR spectroscopy[17] and with interpretations of ^{13}C chemical shifts[14,20] and resonance Raman spectra.[21]

Conclusion

Multidimensional RFDR spectroscopy will undoubtedly prove useful for investigating the molecular structure of a variety of systems, including high molecular weight or immobilized proteins and nucleic acids. In the case of bR, dipolar distance measurements provide details that are important for elucidating the mechanism by which retinal isomerizations regulate proton transport in bR. At present, a similar strategy using RFDR is being implemented to quantify retinal-to-protein distances in bR samples with other labeling schemes and to measure critical distances in cryotrapped photointermediates.

Although RFDR is well-suited for distance measurements of magnetically dilute spin pairs, in some circumstances, this method may be used to map couplings between multiple spin sites if magnetization exchange between all relevant spins is considered. This latter approach may be timely, given the increasing availability of uniformly ^{13}C labeled biomolecules.

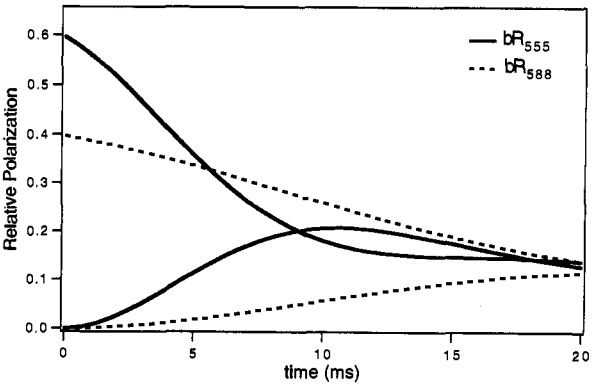

Figure 5. Numerical simulation results showing the magnetization exchange between ε-Lys and 14-retinal as a function of τ_m for bR_{555} (—) and for bR_{568} (- - -). At τ_m = 0, the ε-Lys line has an intensity of 0.6 for bR_{555} and 0.4 for bR_{568}, reflecting the composition of the dark-adapted mixture, and cross-peak intensities are 0. Magnetization exchange is reflected by the decrease in intensity on the diagonal and an increase in intensity of the corresponding cross-peaks. These trajectories are for the dipolar coupling strengths corresponding to distances of 0.31 nm for bR_{555} and 0.39 nm for bR_{568}. Signal losses, which are not shown, account for some decrease in total magnetization (e.g. ~35% loss after 15 ms).

Acknowledgment. This research was supported by the National Institutes of Health (GM23289, GM23403, GM36810, and RR00995), The Netherlands Foundation for Chemical Research (SON), and The Netherlands Organization for the Advancement of Pure Science (NWO). J.M.G. is an American Cancer Society Postdoctoral Fellow (PF-3875). A.E.B. was a recipient of a National Science Foundation Predoctoral fellowship. We thank J. R. Long and D. C. Maus for careful reading of the manuscript.

(19) Donohue, J. *J. Am. Chem. Soc.* **1950**, *72*, 949.
(20) Harbison, G. S.; Smith, S. O.; Pardoen, J. A.; Mulder, P. P. J.; Lugtenburg, J.; Herzfeld, J.; Mathies, R. A.; Griffin, R. G. *Proc. Natl. Acad. Sci. U.S.A.* **1984**, *81*, 1706.
(21) Smith, S. O.; Hornung, I.; van der Steen, R.; Pardoen, J. A.; Braiman, M. S.; Lugtenburg, J.; Mathies, R. A. *Proc. Natl. Acad. Sci. U.S.A.* **1984**, *81*, 2005.
(22) Gullion, T.; Baker, D. B.; Conradi, M. S. *J. Magn. Reson.* **1990**, *89*, 479–482.
(23) (a) Morris, G. A.; Freeman, R. *J. Magn. Reson.* **1978**, *29*, 433–462. (b) Caravatti, P.; Bodenhausen, G.; Ernst, R. R. *J. Magn. Reson.* **1983**, *55*, 88–103.